Article

# Amino Acid-Type Edited NMR Experiments for Methyl–Methyl Distance Measurement in $^{13}$C-Labeled Proteins

Hlne Van Melckebeke, Jean-Pierre Simorre, and Bernhard Brutscher

*J. Am. Chem. Soc.*, **2004**, 126 (31), 9584-9591• DOI: 10.1021/ja0489644 • Publication Date (Web): 17 July 2004



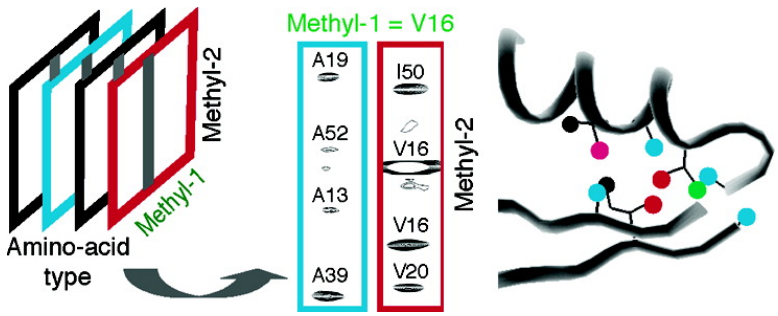


## More About This Article

Additional resources and features associated with this article are available within the HTML version:

- Supporting Information
- Links to the 2 articles that cite this article, as of the time of this article download
- Access to high resolution figures
- Links to articles and content related to this article
- Copyright permission to reproduce figures and/or text from this article

View the Full Text HTML

J|A|C|S
ARTICLES
Published on Web 07/17/2004

# Amino Acid-Type Edited NMR Experiments for Methyl−Methyl Distance Measurement in $^{13}$C-Labeled Proteins

Hélène Van Melckebeke, Jean-Pierre Simorre, and Bernhard Brutscher*

*Contribution from the Institut de Biologie Structurale, Jean-Pierre Ebel CNRS-CEA-UJF, 41, rue Jules Horowitz, 38027 Grenoble Cedex, France*

Received February 24, 2004; E-mail: Bernhard.Brutscher@ibs.fr

***Abstract:*** New NMR experiments are presented for the measurement of methyl−methyl distances in $^{13}$C-labeled proteins from a series of amino acid-type separated 2D or 3D NOESY spectra. Hadamard amino acid-type encoding of the proximal methyl groups provides the high spectral resolution required for unambiguous methyl−methyl NOE assignment, which is particularly important for fast global fold determination of proteins. The experiments can be applied to a wide range of protein systems, as exemplified for two small proteins, ubiquitin and MerAa, and the 30 kDa BRP−Blm complex.

## Introduction

Liquid-state NMR spectroscopy has been established as a powerful method for structure determination of proteins. The development of many multidimensional triple-resonance NMR experiments over the past decade, combined with advanced isotope-labeling strategies, has significantly enlarged the scope of NMR problems that can now be studied by NMR. On one hand, TROSY-type experiments[1] have increased the size of molecules amenable to an NMR investigation. Recently, near-complete backbone assignments have been reported for the 723-residue malate synthase G protein from *Escherichia coli*,[2] the 110 kDa homo-octameric protein 7,8-dihydroneolpterin aldolase,[3] and the membrane proteins OmpX and OmpA.[4] On the other hand, the development of new acquisition schemes has sped up NMR data collection.[5] Such techniques are especially promising in the context of fast NMR fold determination of moderately sized proteins (<200 residues). Recently, we have obtained complete backbone and methyl side-chain assignment of two proteins, the 68-residue protein fragment MerAa from *Ralstonia metallidurans* and the 167-residue protein fragment SiR−FP18 from *E. coli*, from a set of two-dimensional NMR spectra acquired in an overall experimental time of less than 48 h.[6,7] With these experimental advances, the most limiting and time-consuming step of the NMR structure determination process remains the measurement and unambiguous assignment of NOE cross-peaks to specific, proximal pairs of protons.

Methyl groups are extremely valuable probes of molecular structure and dynamics. Methyl-containing residues are generally well-dispersed throughout the primary sequence, and the methyl groups are preferably located in the hydrophobic protein core. Therefore, methyl−methyl distances derived from NOE measurements provide a rich source of long-range structural information.[8] For NMR studies, methyls are advantageous because they give rise to reasonably well-resolved $^{1}$H−$^{13}$C correlation spectra with good sensitivity even for larger molecules.[9] The high sensitivity of methyl correlation experiments, as compared to that of CH or $CH_2$ groups, is explained by favorable $^{1}$H and $^{13}$C transverse relaxation due to the fast methyl rotation and the presence of three equivalent protons attached to the methyl carbon. In addition, robust labeling strategies developed for obtaining uniformly deuterated proteins with protonated methyl groups[10] allow application of methyl-based NMR methods to high molecular weight systems. Methyl resonance assignments have been obtained for molecular systems with a tumbling correlation time of up to 20 ns[11] using standard $^{13}$C-TOCSY-based magnetization transfer experiments. More recently, Kay and co-workers have achieved near-complete methyl assignments for Ile, Val, and Leu side chains of the 723-

(1) Pervushin, K.; Riek, R.; Wider, G.; Wüthrich, K. *Proc. Natl. Acad. Sci. U.S.A.* **1997**, *94*, 12366−12371.
(2) Tugarinov, V.; Muhandiram, R.; Ayed, A.; Kay, L. E. *J. Am. Chem. Soc.* **2002**, *124*, 10025−10035.
(3) Salzmann, M.; Pervushin, K.; Wider, G.; Senn, H.; Wüthrich, K. *J. Am. Chem. Soc.* **2000**, *122*, 7543−7548.
(4) (a) Fernandez, C.; Hilty, C.; Bonjour, S.; Fernandez, C.; Pervushin, K.; Wüthrich, K. *FEBS Lett.* **2001**, *504*, 173−178. (b) Fernandez, C.; Fernandez, C.; Wüthrich, K. *Proc. Natl. Acad. Sci. U.S.A.* **2001**, *98*, 2358−2363. (c) Arora, A.; Abilgaard, F.; Bushweller, J. H.; Tamm, L. K. *Nat. Struct. Biol.* **2001**, *8*, 334−338.
(5) (a) Freeman, R.; Kupce, E. *J. Biomol. NMR* **2003**, *27*, 101−113. (b) Kupce, E.; Nishida, T.; Freeman, R. *Prog. Nucl. Magn. Reson. Spectrosc.* **2003**, *42*, 95−122.
(6) (a) Bersch, B.; Rossy, E.; Covès, J.; Brutscher, B. *J. Biomol. NMR* **2003**, *27*, 57−67. (b) Brutscher, B. *J. Biomol. NMR* **2004**, *29*, 57−64.
(7) Brutscher, B. *J. Magn. Reson.* **2004**, *167*, 178−184.
(8) (a) Rosen, M. K.; Gardner, K. H.; Willis, R. C.; Parris, W. E.; Pawson, T; Kay, L. E. *J. Mol. Biol.* **1996**, *263*, 627−636. (b) Metzler, W. J.; Wittekind, M.; Goldfarb, V.; Mueller, L.; Farmer, B. T. *J. Am. Chem. Soc.* **1996**, *118*, 6800−6901. (c) Mueller, G. A.; Choy, W. Y.; Yang, D.; Forman-Kay, J. D.; Venters, R. A.; Kay, L. E. *J. Mol. Biol.* **2000**, *300*, 197−212.
(9) Gardner, K. H.; Rosen, M. K.; Kay, L. E. *Biochemistry* **1997**, *36*, 1389−1401.
(10) (a) Gardner, K. H.; Kay, L. E. *Annu. Rev. Biophys. Biomol. Struct.* **1998**, *27*, 357−406. (b) Goto, N. K.; Gardner, K. H.; Mueller, G. A.; Willis, R. C.; Kay, L. E. *J. Biomol. NMR* **1999**, *13*, 369−374.
(11) (a) Gardner, K. H.; Zhang, X.; Gehring, K.; Kay, L. E. *J. Am. Chem. Soc.* **1998**, *120*, 11738−11748. (b) Hilty, C.; Fernandez, C.; Wider, G.; Wüthrich, K. *J. Biomol. NMR* **2002**, *23*, 289−301.


**10.1021/ja0489644 CCC: $27.50** 

residue malate synthase G protein using a new isotopic labeling strategy in combination with a set of COSY-type transfer experiments.[12] $^{13}$C-edited NOESY experiments using constant time (CT) $^{13}$C frequency labeling have been proposed in the past[13] to record high-resolution methyl−methyl correlation spectra. Such experiments have been successfully applied to fully or methyl-only protonated protein samples in the molecular weight range of up to 40 kDa. The main limitations of the experiment of Zwahlen et al.[13] are that it does not allow fast data collection and that the spectral resolution may still not be sufficient for unambiguous NOE assignment in the case of larger molecules. As demonstrated here, these limitations may be overcome by the addition of amino acid-type editing filters to the original sequence, which spreads the methyl−methyl correlation peaks along additional dimensions according to the amino acid type of the methyl-containing residue.

In this article, we propose new $^{13}$C-edited HSQC−NOESY−HSQC-type experiments, where one amino acid-type editing filter is added to the standard $^1$H and $^{13}$C frequency dimensions for each of the two methyls involved in the NOE interaction. This yields ($n_{cs} + n_{aa}$)-dimensional NOESY spectra, with $n_{cs}$ and $n_{aa}$ the number of chemical shift and amino acid-type dimensions, respectively. These amino acid-type edited methyl NOESY experiments are equally useful for application to small and large molecular systems. For smaller molecules, ($2_{cs} + 2_{aa}$)-D methyl NOESY spectra are recorded in a short acquisition time, typically a few hours on a modern high field NMR spectrometer. In these spectra, one of the proximal methyl groups is labeled by its $^{13}$C frequency and amino acid type, whereas the other one is identified by its $^1$H frequency and amino acid type. The resulting ($2_{cs} + 2_{aa}$)-D NOESY correlation maps provide a set of mostly unambiguous methyl−methyl distance restraints, which is important for the validation of a structural homology model or for de novo protein fold determination. The amino acid-type selective methyl NOESY experiment is demonstrated on $^{13}$C, $^{15}$N-labeled samples of two small proteins: (i) MerAa, a protein fragment consisting of the 68 N-terminal residues of the cytosolic mercuric reductase MerA from *R. metallidurans* and (ii) the 76-residue *human* ubiquitin. For the two proteins, the set of intermethyl distance restraints extracted from the ($2_{cs} + 2_{aa}$)-D NOESY spectra, recorded in a short experimental time, proved sufficient for molecular fold determination. For larger molecular systems, acquisition of ($3_{cs} + 1_{aa}$)-D or ($3_{cs} + 2_{aa}$)-D correlation maps provides the necessary spectral resolution for methyl−methyl NOE assignment and an attractive spectroscopic alternative to amino acid-type selective isotope labeling approaches. Such spectra can still be recorded in a reasonable experimental time of a few days, thus presenting an attractive way of collecting long-range distance restraints of larger protein systems with assigned methyl resonances. A ($3_{cs} + 1_{aa}$)-D methyl NOESY spectrum, acquired on a $^{13}$C, $^{15}$N-labeled sample of the 30 kDa bleomycine-resistance protein−bleomycine ($Zn^{2+}$) complex (BRP−Blm) from *Streptoalloteichus hindustanus*, demonstrates the performance of the new experiment for application to larger molecular systems.

## Materials and Methods

**NMR Samples.** Uniformly $^{13}$C, $^{15}$N-labeled *human* ubiquitin was purchased from VLI (Southeastern, PA). A sample was prepared containing 2 mM ubiquitin in 45 mM sodium acetate buffer at pH 4.7 (90% $H_2O$, 10% $D_2O$). $^{13}$C, $^{15}$N-labeled MerAa from *R. metallidurans* was prepared as described previously.[30] Sample conditions were 1.5 mM protein in 50 mM Tris buffer at pH 7 (90% $H_2O$, 10% $D_2O$). A total of 1.2 molar equivalent of $HgCl_2$ was added to form the metal−protein complex. A $^{13}$C, $^{15}$N-labeled sample of the complex between *S. hindustanus* Bleomycin resistance protein (BRP) and $Zn^{2+}$-ligated bleomycine (Blm) was prepared as described previously.[14] The final BRP−Blm concentration was 1 mM in 20 mM deuterated MES buffer at pH 6.5 (∼99% $D_2O$), supplemented with 100 mM NaCl and 0.02% sodium azide.

**NMR Data Acquisition and Processing.** All NMR experiments were performed on a Varian INOVA 800 spectrometer, equipped with a triple-resonance ($^1$H, $^{15}$N, $^{13}$C) probe and shielded three-axes gradients. Additional ($2_{cs} + 1_{aa}$)-D CT-HSQC spectra were acquired on a Varian INOVA 600 spectrometer to calibrate the Bloch-Siegert frequency shifts at 600 MHz $^1$H frequency. The sample temperature was set to 25 °C for MerAa and to 30 °C for ubiquitin and the BRP−Blm complex. Data processing and determination of peak positions were performed using the FELIX program version 2000 (Accelrys, Inc.). Mirror image linear prediction[15] was applied to the $^{13}$C CT dimensions. Squared cosine apodization was used in all dimensions prior to zero-filling and Fourier transformation.

For the ($2_{cs} + 1_{aa}$)-D CT-HSQC spectra recorded for ubiquitin and MerAa, the pulse sequence of Figure 1a was used without the NOE mixing and the second $^1$H−$^{13}$C HSQC transfer bloc. Data sets of 4 times ($AA_i$) 110($^{13}$C) × 512($^1$H) complex points were recorded for spectral widths of 4000 Hz ($^{13}$C) and 9000 Hz ($^1$H) in an overall experimental time of 30 min.

The amino acid-type editing filters were implemented using continuous $C^{next}$ band-selective decoupling. As shown in Figure 1 dilated evolution times, $\lambda^n t_1$ and $\lambda^n t_2$ were used to compensate Bloch-Siegert shifts induced by the band-selective $C^{next}$-decoupling. The $B_0$ field-dependent scaling factors $\lambda^n$ were calibrated experimentally from ($2_{cs} + 1_{aa}$)-D CT-HSQC spectra of ubiquitin and MerAa recorded at two $B_0$ field strengths of 14.4T and 18.8T, corresponding to $^1$H frequencies of 600 and 800 MHz. The following optimized scaling factors were used for the four Hadamard experiments $H_4(n)$: $\lambda_{600}{}^1 = 1.0$, $\lambda_{600}{}^2 = 1.0046$, $\lambda_{600}{}^3 = 1.0181$, and $\lambda_{600}{}^4 = 1.0162$ at 600 MHz, and $\lambda_{800}{}^1 = 1.0$, $\lambda_{800}{}^2 = 1.0026$, $\lambda_{800}{}^3 = 1.0102$, and $\lambda_{800}{}^4 = 1.0091$ at 800 MHz. The same $C^{next}$-decoupling patterns and scaling factors were then used

(12) Tugarinov, V.; Kay, L. E. *J. Am. Chem. Soc.* **2003**, *125*, 13868−13878.
(13) Zwahlen, C.; Gardner, K. H.; Siddharta, P. S.; Horita, D. A.; Byrd, R. A.; Kay, L. E. *J. Am. Chem. Soc.* **1998**, *120*, 7617−7625.
(14) Vanbelle, C.; Brutscher, B.; Blackledge, M.; Muhle-Goll, C.; Rémy, M.-H.; Masson, J.-M.; Marion, D. *Biochemistry* **2003**, *42*, 651−663.
(15) Zhu, G; Bax, A *J. Magn. Reson.* **1990**, *90*, 405−410.
(16) Weigelt, J.; Hammarström, A.; Bermel, W.; Otting, G. *J. Magn. Reson.* **1996**, *110B*, 219−224.
(17) (a) Clore, G. M.; Kay, L. E.; Bax, A.; Gronenborn, A. M. *Biochemistry* **1991**, *130*, 12−18. (b) Zuiderweg, E. R. P.; Petros, A. M.; Fesik, S. W.; Olejniczak, E. T. *J. Am. Chem. Soc.* **1991**, *113*, 370−371.
(18) (a) Schubert, M.; Oschkinat, H.; Schmieder, P. *J. Magn. Reson.* **2001**, *148*, 61−72. (b) Dötsch, V.; Oswald, R. E.; Wagner, G. *J. Magn. Reson.* **1996**, *110B*, 107−111.
(19) Hadamard, J. *Bull. Sci. Math.* **1893**, *17*, 240−248.
(20) Kupce, E.; Freeman, R. *J. Magn. Reson.* **1996**, *118A*, 299−303.
(21) Kupce, E.; Boyd, J.; Campbell, I D. *J. Magn. Reson.* **1995**, *106B*, 300−303.
(22) Kupce, E.; Freeman, R; Wider, G.; Wüthrich, K. *J. Magn. Reson.* **1996**, *122A*, 81−84.
(23) Zhang, S.; Gorenstein, D. G. *J. Magn. Reson.* **1999**, *138*, 281−287.
(24) Millet, O.; Muhandiram, D. R.; Skrynnikov, N. R.; Kay, L. E. *J. Am. Chem. Soc.* **2002**, *124*, 6439−6448.
(25) Hajduk, P. J.; Augeri, D. J.; Mack, J.; Mendoza, R.; Yang, J.; Betz, S. F.; Fesik, S. W. *J. Am. Chem. Soc.* **2000**, *122*, 7898−7904.
(26) Tjandra, N.; Bax, A. *J. Magn. Reson.* **1997**, *124*, 512−515.
(27) Sibille, N.; Bersch, B.; Covès, J.; Blackledge, M.; Brutscher, B. *J. Am. Chem. Soc.* **2002**, *124*, 14616−14625.
(28) Pervushin, K.; Vögeli, B. *J. Am. Chem. Soc.* **2003**, *125*, 9566−9567.
(29) Meissner, A.; Sørensen, O. W. *J. Biomol. NMR* **2001**, *19*, 69−73.
(30) Rossy, E.; Champier, L.; Bersch, B.; Brutscher, B.; Blackledge, M.; Covès, J. *J. Biol. Inorg. Chem.* **2004**, *9*, 49−58.

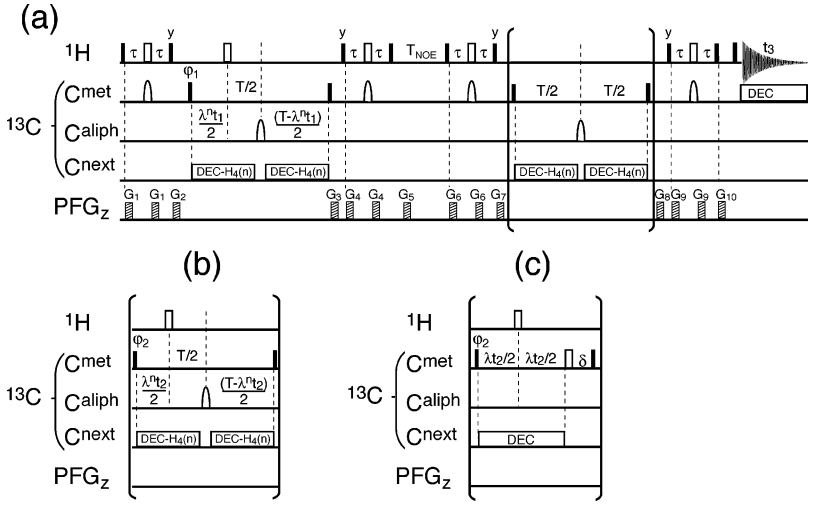


***Figure 1.*** Pulse sequences for amino acid-type edited ($n_{cs} + n_{aa}$)-D methyl NOESY experiments. The pulse sequence in (a) allows recording of ($2_{cs} + 2_{aa}$)-D NOESY spectra. Higher-dimensional experiments, ($3_{cs} + 1_{aa}$)-D or ($3_{cs} + 2_{aa}$)-D NOESY, are generated by inserting one of the pulse sequence blocks labeled (b) and (c) into the brackets of sequence (a). All radio frequency (rf) pulses are applied along the *x*-axis unless indicated. 90° and 180° rf pulses are represented by filled and open pulse symbols, respectively. The proton carrier is set to the water resonance (4.7 ppm), and the $^{13}$C carrier is set to the center of the methyl region (19 ppm) throughout the experiment. $^{13}$C pulses drawn on the $C^{aliph}$ or $C^{next}$ lines are frequency-shifted to 35 ppm ($C^{aliph}$) and the center of the corresponding $C^{next}$ bands, respectively, by a linear phase ramp. The selective 180° $C^{met}$ pulses are applied with an i-SNOB-5 shape[21] covering a bandwidth of 18 ppm. For application at high magnetic field strengths, an offset-compensating $C^{aliph}$ refocusing pulse $58_x{-}140_{-x}{-}344_x{-}140_{-x}{-}58_x$[32] is used during the CT delays $T$ to properly invert all $C^{met}$ and $C^{next}$ carbon spins over a bandwidth of 80 ppm. The CT delay was set to $T = 28$ ms, and the INEPT transfer delays were set to $\tau = 1.6$ ms. The small delay $\delta$ in (c) compensates for the length of the 180° $^1$H pulse. $^{13}$C decoupling during acquisition is achieved using a WALTZ-16 sequence[33] at a field strength of $\gamma B_1/2\pi = 3$ kHz. Pulsed field gradients, $G_{1-G10}$, are applied along the *z*-axis ($PFG_z$) with a gradient strength of approximately 20 G/cm and lengths ranging from 100 to 500 $\mu$s, followed by a recovery delay of 100 $\mu$s. The phase cycle employed is $\varphi_1 = x,-x$, and $\varphi_{rec} = x,-x$. Quadrature detection in $t_1$ and $t_2$ is obtained by incrementing the phases $\varphi_1$ and $\varphi_2$ according to STATES-TPPI. Constant-adiabaticity (CA) WURST-2 pulses are used as the basic elements for the $C^{next}$-decoupling. The CA-WURST-2 pulses have a length of $\tau_p = 5$ ms and cover a bandwidth of 12 ppm. They are centered at 37(1), 53 (−15), and 70 ppm (−32 ppm) for the Val-Ile$_\gamma$, Ala, and Thr $C^{next}$ bands, respectively. The values in parentheses indicate the center of the symmetric off-resonance decoupling applied for each band using the same amplitude modulation but opposite frequency sweep.[22] Multiple-band-selective decoupling is achieved by vector addition of the individual WURST pulses.[34] The final decoupling sequence is phase-cycled according to a TPG-5 supercycle.[35] The $C^{next}$-decoupling is restarted at the beginning after the 180° $C^{aliph}$ refocusing pulse. For the four-step Hadamard amino acid-type selection filter, four experiments are recorded using $C^{next}$-decoupling of different bands: $H_4(1)$ none, $H_4(2)$ Ala and Thr, $H_4(3)$ Ala and (Val-Ile$_\gamma$), $H_4(4)$ Thr and (Val-Ile$_\gamma$). At 800 MHz $^1$H frequency, the scaling factors $\lambda_{800}{}^n$ were set to $\lambda_{800}{}^1 = 1.0$, $\lambda_{800}{}^2 = 1.0026$, $\lambda_{800}{}^3 = 1.0102$, and $\lambda_{800}{}^4 = 1.0091$. At 600 MHz $^1$H frequency, the following optimized scaling factors were used: $\lambda_{600}{}^1 = 1.0$, $\lambda_{600}{}^2 = 1.0046$, $\lambda_{600}{}^3 = 1.0181$, and $\lambda_{600}{}^4 = 1.0162$. A Hadamard transformation[5,19] is applied along the filter dimensions to disentangle the NMR signals from the individual frequency bands. $C^{next}$-decoupling during $t_2$ in (c) is realized using the same WURST-2 based sequence described above applied to the Ala, Thr, and (Val-Ile$_\gamma$) $C^{next}$-frequency bands simultaneously. Bloch-Siegert shift compensation is achieved by setting $\lambda_{800} = 1.0111$ (or $\lambda_{600} = 1.0195$). For modulation sideband suppression the decoupling sequence is shifted in time by an amount of $\tau_p/2$ for each second scan.[16] Pulse sequences in Varian pulse sequence language and transformation protocols in Felix macro language can be obtained from the authors upon request.

without any further optimization for the amino acid-type edited NOESY experiments, described below.

($2_{cs} + 2_{aa}$)-D methyl NOESY spectra were recorded using the pulse sequence of Figure 1a. Different NOE mixing times were tested ranging from 75 to 200 ms. The highest NOE cross-peak intensities were observed in the spectra recorded with $T_{NOE} = 200$ ms. Four-step amino acid-type editing was used during the two CT $^{13}$C-evolution periods before and after the NOE mixing. Chemical shift evolution was sampled with 110($t_1$) and 512($t_3$) complex points for spectral widths of 4000 and 9000 Hz, respectively, yielding a final matrix of 220($C_i$) × 1024($H_j$) × 4($AA_i$) × 4($AA_j$) data points. The total acquisition time was set to 2 h for ubiquitin and 4 h for MerAa.

A ($3_{cs} + 1_{aa}$)-D methyl NOESY spectrum was acquired for the BRP−Blm complex using the pulse sequence of Figure 1a with the insert of Figure 1c. The NOE mixing time was set to 100 ms. Multiple-band-selective $C^{next}$-decoupling was applied during $t_2$ using two different decoupling schemes for alternating scans.[16] Chemical shift evolution was sampled with 90($t_1$), 90($t_2$), and 512($t_3$) complex points for spectral widths of 4000 ($C_i$), 4000 ($C_j$), and 9000 Hz ($H_j$), respectively, yielding a final matrix of 180($C_i$) × 180 ($C_j$) × 1024 ($H_j$) × 4($AA_i$) data points. A simple two-step phase cycle, two scans per FID, and a repetition delay of 0.9 s were used to yield a total acquisition time of 80 h.

## Results and Discussion

Figure 1 illustrates the new $^{13}$C and amino acid-type edited methyl NOESY experiment developed to record high-resolution NOESY spectra for methyl−methyl distance measurement. The pulse sequence is of the $^{13}$C-HSQC-NOESY-$^{13}$C-HSQC type[13,17] with the flow of magnetization for two proximal methyl groups (i) and (j) given as follows:

$$H_i \xrightarrow{J_{CH}} C_i[t_1,AA_i - \text{filter}] \xrightarrow{J_{CH}} H_i \xrightarrow{NOE} H_j \xrightarrow{J_{CH}} C_j[t_2,AA_j - \text{filter}] \xrightarrow{J_{CH}} H_j[t_3] \quad (1)$$

The active spin−spin couplings are indicated above the arrows. While $C_i$ frequency labeling is performed in a CT manner during $t_1$, with the constant time delay set to the inverse of the scalar carbon−carbon coupling constant ($T \cong 1/J_{CC}$), for $C_j$ either CT (Figure 1b), real-time (Figure 1c), or no (Figure 1a) frequency labeling is used in $t_2$. Two AA filters can be applied, one before and one after the NOE mixing, thus allowing additional amino acid-type identification of both interacting methyl groups. The pulse sequence of Figure 1a allows recording of fast ($2_{cs} + 2_{aa}$)-D ($C_i$, $AA_i$, $H_j$, $AA_j$)-NOESY spectra for application to small and medium-sized proteins under high-sensitivity experimental conditions (concentrated protein sample, high magnetic field strength, cryogenic probe, etc.). For application to larger proteins, both methyl carbons $C_i$ and $C_j$

are frequency-labeled, using the inserts of Figure 1b or 1c to record ($3_{cs} + 2_{aa}$)-D ($C_i$, $AA_i$, $C_i$, $H_j$, $AA_j$)-NOESY or ($3_{cs} + 1_{aa}$)-D ($C_i$, $AA_i$, $C_i$, $H_j$)-NOESY spectra, respectively. The major modification with respect to pulse sequences proposed previously[13] is the addition of amino acid-type editing filters (AA filters), which will be discussed in detail in the following section.

**Amino Acid-Type Editing of Methyl Groups.** Amino acid-type selective experiments have been proposed in the past[18] to simplify the $^1H-^{15}N$ correlation spectra of $^{13}C,^{15}N$ labeled proteins. These experiments exploit the different spin-coupling topologies of amino acid side chains. Here, a different concept is used for amino acid-type editing based on frequency-selective Hadamard spectroscopy.[5,19] Methyl groups are located at the side-chain ends, and thus the methyl $C^{met}$ is only bound to one other carbon, which we will refer to as $C^{next}$. The $C^{next}$ corresponds to carbon sites with distinct chemical shift ranges for different amino acid types. This feature is exploited in the Hadamard amino acid-type selection filters of Figure 1. Four $C^{next}$ frequency bands were defined as follows: AA = 4: 64−76 ppm (Thr), AA = 3: 31−43 ppm (Val-Ile-$\gamma$), AA = 2: 47−59 ppm (Ala), and AA = 1: 10−30 ppm (Leu-Ile$_\delta$). The $^{13}C$ spins resonating within these frequency bands can be manipulated independently by means of band-selective radio frequency (rf) pulses. A binary Hadamard-type $C^{next}$-frequency encoding scheme, consisting in a series of "plus" and "minus" signs, is used to disperse the methyl correlations along an additional amino acid-type dimension. The sign encoding is realized by the presence ("minus") or absence ("plus") of $C^{met} - C^{next}$ scalar-coupling ($J_{CC}$) evolution during the CT delay $T$. In the absence of $C^{next}$-decoupling, the $J_{CC}$ coupling evolution is active during $T = 1/J_{CC}$, resulting in a sign inversion of the detected NMR signal ("minus"-encoding):

$$C_x^{met} \xrightarrow{J_{CC}} - C_x^{met}$$

Additional band-selective $C^{next}$-decoupling allows switching off the $C^{met} - C^{next}$ scalar coupling evolution for a given amino acid type ("plus"-encoding):

$$C_x^{met} \xrightarrow{dec} + C_x^{met}$$

Four spectra are recorded, where the sign of the NMR signals originating from methyl groups with $C^{next}$ corresponding to different frequency bands is changed according to a Hadamard matrix of order 4: $H_4(1)$: without $C^{next}$-decoupling, $H_4(2)$: with Ala-Thr $C^{next}$-decoupling, $H_4(3)$: with Ala-(Val-Ile$_\gamma$) $C^{next}$-decoupling, and $H_4(4)$: with Thr-(Val-Ile$_\gamma$) $C^{next}$-decoupling. The four bands (AA = 1, 2, 3, and 4), corresponding to different amino acid types, are then disentangled by a Hadamard transformation performing linear combinations of the four recorded data sets $H_4(1)$, ..., $H_4(4)$. In this Hadamard filter, the methionine methyl groups, which have no directly attached carbon, are detected in the AA = 1 band together with the methyls from Leu and Ile$_\delta$ residues, but with negative intensity. Hadamard spectroscopy provides a time-saving alternative to $C^{next}$ chemical shift labeling along an additional frequency dimension, because only four points need to be recorded for the Hadamard AA-type dimension. It is also more sensitive because no additional spin evolution period is required, and the full NMR signal is detected (sign-modulated) in each of the four Hadamard experiments. Therefore, the amino acid-type edited $^1H-^{13}C$ correlation experiment retains the full sensitivity of the conventional experiment of the same duration.

$C^{next}$-decoupling can be achieved in two alternative ways: either by continuous band-selective decoupling or by band-selective spin inversion. The latter implementation has the advantage that no Bloch-Siegert shifts or modulation sidebands are created, but it reduces the available time for $C^{met}$ chemical shift labeling, and thus the spectral resolution. We have tested both approaches experimentally, using a 5 ms constant adiabaticity (CA) WURST-2 pulse[20] as the repeated element of the decoupling sequence and an i-SNOB-5[21] pulse shape for $C^{next}$ spin inversion. We obtained a much better filter performance (proper selection of the individual AA bands) in the case of continuous band-selective decoupling, provided that the Bloch-Siegert shifts and modulation sidebands were correctly suppressed. Therefore, we have chosen the continuous decoupling option for all the experiments presented here. Bloch-Siegert shift compensation is crucial for the amino acid-type editing filter, which relies on the addition and subtraction of different subspectra. Additional off-resonance decoupling is applied for each $C^{next}$ band, symmetrically with respect to the center of the methyl spectrum with the same shape and opposite frequency sweep.[22] This eliminates the Bloch-Siegert shifts for $C^{met}$ resonances close to the spectral center. The remaining shifts, which are a linear function of the $C^{met}$ frequency offset, can be compensated by appropriately adjusting the $B_0$-field-dependent scaling factors $\lambda^n$ in the pulse sequence of Figure 1.[23] Experimentally optimized $\lambda_{600}{}^n$ and $\lambda_{800}{}^n$ values are given in the Materials and Methods section and in the caption to Figure 1. Modulation sidebands are suppressed by properly adjusting the WURST-2 pulse length and the constant time delay $T$. A detailed theoretical and experimental evaluation of these effects on the filter performance is presented elsewhere (Van Melckebeke, H.; Simorre, J.-P.; Brutscher, B. *J. Magn. Reson.* **2004**, in press).

To demonstrate the performance of the new amino acid-type methyl-editing filter, a ($2_{cs} + 1_{aa}$)-D CT-HSQC spectrum was recorded on the MerAa sample. The ($C_i$, $H_i$, $AA_i$) correlation spectrum was acquired using the pulse sequence of Figure 1a without the NOE mixing and the second $^1H-^{13}C$ HSQC transfer block. The four 2D planes extracted along the $AA_i$ dimension are shown in Figure 2a−d. A few small residual peaks (marked by a star) are observed in the spectra of Figure 2a,c with an intensity of less than 5% of the normal cross-peak intensity. These peaks are due to slightly different peak intensities of the particular cross-peak in the four data sets recorded for the filter, because of small variations in the $J_{CC}$ coupling constants and differential relaxation of $C_x^{met}$ and $2C_x^{met}C_z^{next}$ coherence. A clean separation of methyls from Ala and Thr side chains is obtained by the filter sequence. While the alanine (AA = 2) and threonine (AA = 4) bands cover more than 95% of the corresponding $C^{next}$ chemical shifts found for diamagnetic proteins in the BMRB data bank, only about 70% of the valine and 85% of the Ile$_\gamma$ methyls have their corresponding $C^{next}$ frequencies inside the AA = 3 band. This leads to some "cross-talk" between the AA = 1 (Met-Leu-Ile$_\delta$) and AA = 3 (Val-Ile$_\gamma$) bands, as shown in Figure 2a,c for MerAa. Therefore, some ambiguities may remain when using such methyl correlation spectra for amino acid-type identification.

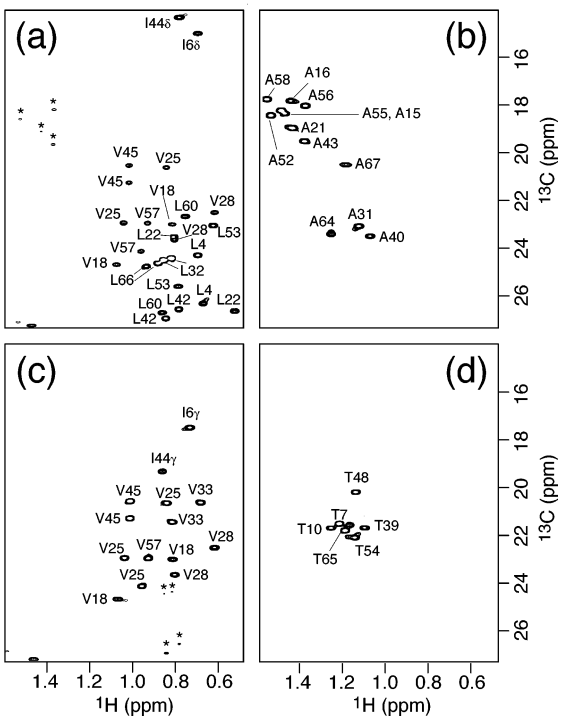


***Figure 2.*** ($2_{cs} + 1_{aa}$)-D methyl CT-HSQC spectrum recorded for MerAa using the pulse sequence of Figure 1a without the NOE mixing and the second HSQC. The four ($C_i$, $H_i$) spectra extracted along the Hadamard filter dimension are shown in (a) (Met-Leu-Ile$_\delta$) band, (b) Ala band, (c) (Val-Ile$_\gamma$) band, and (d) Thr band. The corresponding amino acid type and residue number assigns the bona fide cross-peaks, and a star indicates a residual peak due to filter imperfections.

In conclusion, spectral resolution of the methyl $^{1}$H−$^{13}$C correlation spectrum is significantly enhanced by the amino acid-type selection filter, without a significant increase in experimental time. We therefore expect that the amino acid-type editing filter, presented here, will improve many existing NMR experiments based on the resolution of $^{1}$H−$^{13}$C methyl correlation spectra, especially for application to larger molecules. Examples are the study of side-chain dynamics,[24] molecular interfaces by chemical shift mapping,[25] or the measurement of residual dipolar or scalar coupling constants for structure determination.[26−28]

**Application to Smaller Molecules: Fast Methyl NOE Measurement.** As a first application of interest, highly resolved methyl ($2_{cs} + 2_{aa}$)-D NOESY spectra of moderately sized proteins can be recorded in a short experimental time, using the pulse sequence of Figure 1a. Acquisition times of 2 h for ubiquitin and 4 h for MerAa proved sufficient on a standard 800 MHz spectrometer to detect a large number of methyl−methyl correlation peaks. The experiment is basically a 2D NOESY experiment where one of the proximal methyls (methyl-i) is identified by its $^{13}$C, and the other one (methyl-j) is identified by its $^{1}$H frequency. CT $^{13}$C editing removes line splitting due to scalar $J_{CC}$ couplings yielding narrow lines. In general, such 2D ($C_i$, $H_j$)-NOESY spectra suffer from the presence of strong diagonal peaks with intensities 1 order of magnitude higher than observed for the cross-peaks and, in addition, from severe signal overlap among cross-peaks. Both problems were addressed in the present experiment by amino acid-type spectral editing filters, described in the previous section, and applied before and after the NOE mixing. In the resulting ($2_{cs} + 2_{aa}$)-D spectrum, the NOE diagonal and cross-peaks are spread along two additional dimensions ($AA_i$, $AA_j$) according to the amino acid-type of the involved methyl groups (see above). Diagonal peaks are detected in only four out of the 16 ($C_i$, $H_j$) planes, while the 12 remaining planes are (mostly) diagonal-free. The concept of double-editing for diagonal suppression has been proposed in the past for $CH_n$-multiplicity editing in HCCH correlation spectra of proteins.[29] Examples of 2D ($C_i$, $H_j$) planes, extracted from the ($2_{cs} + 2_{aa}$)-D NOESY spectrum of MerAa at different ($AA_i$, $AA_j$) coordinates, are shown in Figure 3a−c. The observed correlation peaks correspond to NOEs between methyl groups of Ala and either (a) Val-Ile$_\gamma$, (b) Met-Leu-Ile$_\delta$, or (c) Thr residues. Most of the peaks are well-resolved, and the few residual diagonal peaks (indicated by a star in Figure 3) are of the same or lower intensity than the observed cross-peaks. The high spectral resolution allows fast and straightforward NOE peak assignment. The remaining ambiguities are resolved by exploiting the intrinsic symmetry of the methyl NOESY spectrum. The spatial proximity of two methyls gives rise to a first cross-peak at ($C_i$, $H_j$, $AA_i$, $AA_j$) and a second one at ($C_j$, $H_i$, $AA_j$, $AA_i$) in the ($2_{cs} + 2_{aa}$)-D NOESY data set. A simple protocol allows extraction of (almost) unambiguous methyl−methyl distance restraints from peak picking lists of the ($2_{cs} + 2_{aa}$)-D NOESY data set and the assigned ($2_{cs} + 1_{aa}$)-D CT-HSQC spectrum (C-program available from the authors upon request). The low time requirement for recording a ($2_{cs} + 2_{aa}$)-D NOESY spectrum also makes it attractive to run a series of experiments varying the NOE mixing time $T_{NOE}$ to detect and quantify a larger number of long-range methyl NOEs.

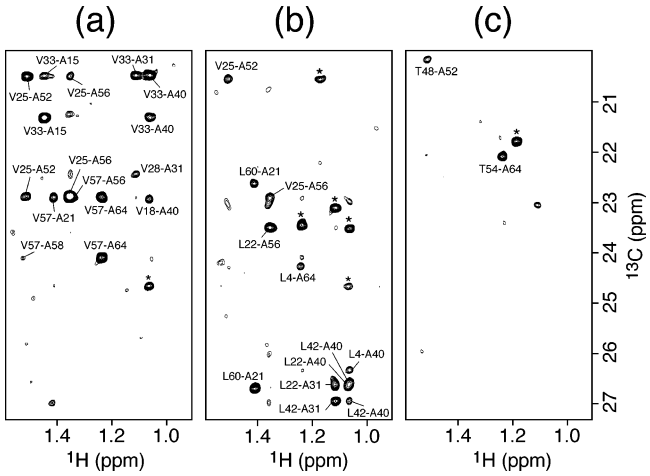


***Figure 3.*** 2D ($C_i$, $H_j$) planes extracted from a ($2_{cs} + 2_{aa}$)-D methyl NOESY spectrum recorded for MerAa using the pulse sequence of Figure 1a. An NOE mixing time of 200 ms was used. The different sub spectra were extracted at (a) $AA_i = 3$, $AA_j = 2$, (b) $AA_i = 1$, $AA_j = 2$, and (c) $AA_i = 3$, $AA_j = 2$, with 1, 2, 3, and 4 corresponding to the (Met-Leu-Ile$_\delta$), Ala, (Val-Ile$_\gamma$), and Thr bands, respectively. Peaks labeled by a star are residual diagonal peaks, whereas assigned peaks correspond to methyl−methyl NOEs.

Figure 4 shows connectivity plots of observed short methyl−methyl distances in the proteins (a) ubiquitin and (b) MerAa. Different symbols represent NOE peaks detected in distinct ($C_i$, $H_j$) planes of the ($2_{cs} + 2_{aa}$)-D NOESY spectra. The cross-peaks were assigned without relying on the existing structures of the two molecules. A total of 52 and 58 medium- and long-range contacts ($i \geq j + 2$) were observed for ubiquitin and MerAa, respectively. A large number of the relevant NOE peaks were

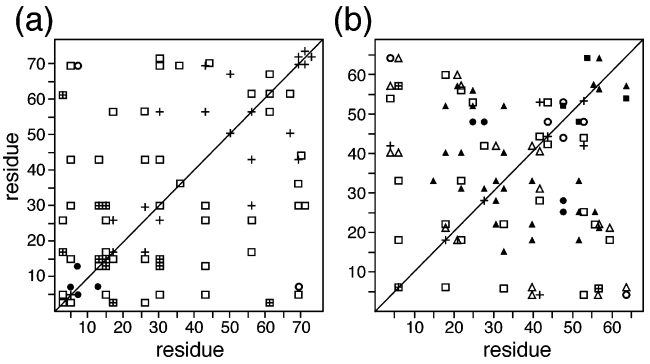


***Figure 4.*** Methyl NOE connectivity plot for (a) ubiquitin and (b) MerAa. All NOEs were extracted and assigned from a single $(2_{cs} + 2_{aa})$-D methyl NOESY spectrum recorded in 2 h for ubiquitin and 4 h for MerAa. The different symbols indicate in which 2D (C, H) planes the particular NOE has been detected: Open triangles (1, 2), open squares (1, 3), open circles (1, 4), filled triangles (2, 3), filled squares (2, 4), filled circles (3, 4), with $(k, l)$ the coordinates $(AA_i = k, AA_j = l)$ in the $(2_{cs} + 2_{aa})$-D methyl NOESY spectrum. The numbers 1, 2, 3, and 4 correspond to the (Met-Leu-Ile$_\delta$), Ala, (Val-Ile$_\gamma$), and Thr bands, respectively. Note that all NOE peaks were also detected in the symmetric $(l, k)$ plane. A cross indicates a diagonal plane $(k, k)$.

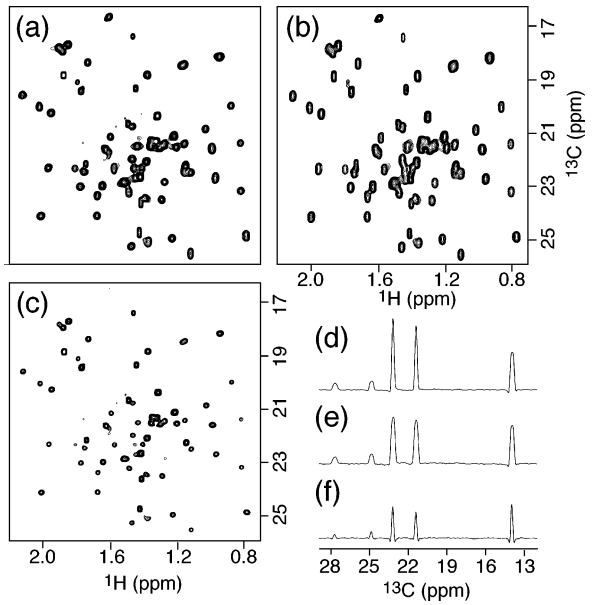


***Figure 5.*** $^1$H$-^{13}$C methyl correlation spectra of the BRP$-$Blm complex recorded at 800 MHz $^1$H frequency using (a) real-time $^{13}$C labeling and C$^{next}$-decoupling of the Ala, (Val-Ile$_\gamma$), and Thr bands, (b) real-time $^{13}$C labeling, and (c) constant time $^{13}$C labeling. Identical acquisition and processing parameters were used for all three experiments. The $t_1$ acquisition time was set to $t_1^{max} = 28$ ms, which ensures reasonably well-resolved correlation spectra even for non-CT frequency labeling. The three spectra were plotted using the same contour levels. For a better appreciation of the relative line width and intensity, 1D spectra were extracted along the $^{13}$C dimension at 0.8 ppm $^1$H frequency from (d) C$^{next}$-decoupled HSQC, (e) HSQC, and (f) CT-HSQC spectra.

extracted from "diagonal-free" NOESY planes. Because of the different amino acid-type composition of the two proteins, the dispersion of the NOE cross-peaks along the additional Hadamard AA dimensions differs for the two proteins. While for MerAa a large number of observed NOEs involve alanine residues, for ubiquitin mostly valine, leucine, and isoleucine residues are found in the hydrophobic protein core. The experiment works well for both proteins, yielding a large number of long-range distance restraints in a short experimental time. The set of proximal methyl$-$methyl contacts obtained for MerAa (Figure 4b) is very similar to previous results obtained from a standard 3D CT-HSQC-NOESY-CT-HSQC data set acquired in an overall time of 60 h,[30] as compared to 4 h for the new $(2_{cs} + 2_{aa})$-D NOESY experiment. Combined with additional restraints defining the local structure of the two $\alpha$-helices and the $\beta$-sheet, the methyl$-$methyl NOEs proved sufficient to define the fold of the protein with an rmsd of $\sim$1.2 Å calculated over the heavy atoms of the protein backbone.[30] Compared to standard 3D NMR techniques, measurement times are reduced by roughly 1 order of magnitude, as long as sensitivity is not the limiting factor. The new $(2_{cs} + 2_{aa})$-D methyl NOESY experiment complements the set of NMR experiments proposed for fast backbone and methyl side-chain resonance assignment.[6,7] This makes it possible to record a complete set of NMR data required for resonance assignment and molecular fold determination in typically a few days or less on a modern high field NMR spectrometer. Fast data acquisition will be particularly important for high-throughput molecular fold screening of small proteins and for the study of unstable protein systems by NMR.

**Application to Larger Molecules: Optimized Resolution and Sensitivity of Methyl NOE Experiments.** For larger proteins, a third chemical shift dimension ($C_j$) is added to the methyl NOE experiment (inserts of Figure 1b,c) to retain the high spectral resolution required for unambiguous NOE assignment. Because the sensitivity of the pulse sequence of Figure 1a decreases very quickly with increasing molecular weight, both sensitivity and spectral resolution of the experiment need to be optimized to detect and unambiguously assign a sufficient number of methyl NOEs for molecular fold determination.

The relative sensitivity of real-time versus CT techniques depends on the molecular tumbling correlation time $\tau_c$ and the total acquisition time $t_1^{max}$.[13] For small molecules or highly mobile side chains, CT $^{13}$C-labeling presents a resolution and sensitivity advantage with respect to real-time frequency labeling because the relaxation loss during the CT delay is compensated by the removal of the line splitting due to the $J_{CC}$ scalar coupling. For larger proteins, CT frequency labeling ensures narrow lines in the $^{13}$C dimensions, albeit at the expense of sensitivity. We have experimentally evaluated the relative sensitivity of $^1$H$-^{13}$C methyl HSQC spectra, using either CT or real-time $^{13}$C labeling, for a sample of the Bleomycin resistance protein (BRP, 2 $\times$ 14 kDa) from *S. hindustanus* in complex with $Zn^{2+}$-ligated bleomycine (Blm). This 30 kDa protein complex was used as a model system for a larger protein. Spectra acquired at 30 °C ($\tau_c = 12.7$ ns) yield an average signal gain of a factor of 1.5 for real time $^{13}$C labeling (Figure 5a,c). At 10 °C ($\tau_c = 22.4$ ns), an average signal enhancement of a factor of 2.5 is obtained (data not shown).

Although the homonuclear $J_{CC}$ couplings are not resolved in the spectra acquired without CT labeling (Figure 5b), they represent a significant contribution to the $^{13}$C line width. Homonuclear decoupling thus offers an attractive way to further increase the resolution and sensitivity of the experiment. C$^{next}$-decoupling during $t_2$ in the pulse sequence element of Figure 1c is applied as described above for the amino acid-type selection filter, with simultaneous decoupling of the Ala, Thr, and (Val-Ile$_\gamma$) bands. Symmetrically applied off-resonance decoupling combined with a dilated evolution time $\lambda t_2$, using

an optimized scaling factor $\lambda$, compensates the Bloch-Siegert shifts in the methyl $^{13}$C spectrum.[23] To suppress the modulation sidebands, a different decoupling sequence is used for odd- and even-numbered scans. As shown previously,[16] the sign of the sidebands can be inverted by a $\tau_p/2$ time shift of one decoupling sequence with respect to the other, where $\tau_p$ is the length of a single inversion pulse as defined above. Addition of the two spectra yields efficient sideband suppression, as illustrated in Figure S1 of the Supporting Information. The C$^{next}$-decoupled $^1$H$-^{13}$C methyl HSQC correlation spectrum, recorded for BRP$-$Blm, is shown in Figure 5a. Compared to the standard HSQC spectrum shown in Figure 5b, a considerable resolution enhancement is observed in the crowded central spectral region that comprises mostly alanine, threonine, valine, and isoleucine-$\gamma$ methyl cross-peaks. This resolution enhancement is accompanied by an increase in signal intensity, which is on average 50%. This gain is slightly reduced to 30% for spectra recorded at 10 °C (data not shown). Cross-peaks from methyl groups in methionine, leucine, and the $\delta$-position of isoleucines are not affected by the C$^{next}$-decoupling. The multiple-band C$^{next}$-decoupled $^1$H$-^{13}$C HSQC sequence (Figure 1c) offers a good compromise between spectral resolution and sensitivity for application to larger proteins, as long as the $J_{CC}$ coupling presents a nonnegligible contribution to the $^{13}$C line width.

The structure of BRP solved by X-ray crystallography[31] and confirmed by solution NMR[14] highlights a homodimeric fold stabilized by an exchanged $\beta$-strand, binding one bleomycine molecule per monomer. BRP is rich in methyl-containing side chains (50 out of 124) resulting in a total of 77 methyl groups per monomer, which are mainly located in the hydrophobic pockets of the protein. The detection of long-range methyl$-$methyl contacts is thus essential for structure determination of this 30 kDa protein complex by NMR. To demonstrate the performance of the new methyl NOESY experiment for application to a larger protein system, we have recorded a $(3_{cs} + 1_{aa})$-D data set of the BRP$-$Blm complex at 30 °C using the pulse sequence of Figure 1a with the insert of Figure 1c. A basic two-step phase cycle allows recording of spectra with high resolution in the $^{13}$C dimensions in a reasonable experimental time of about 3 days. In the $(3_{cs} + 1_{aa})$-D spectrum, one of the proximal methyls is identified by its $^1$H and $^{13}$C chemical shift ($H_i$, $C_i$), whereas the other one is characterized by its $^{13}$C frequency and amino acid type ($C_j$, $AA_j$). A selection of ($\omega_{Ci}$, $\omega_{Hj}$) strips extracted form the $(3_{cs} + 1_{aa})$-D data set is shown in Figure 6a. Each slice is taken at the $\omega_{Cj}$ frequency corresponding to the $^{13}$C chemical shift of the methyl group indicated at the top. Only $AA_i$ slices corresponding to the (Met-Leu-Ile$_\delta$), Ala, and (Val-Ile$_\gamma$) bands are shown, as no threonine residues are found in this particular hydrophobic patch (Figure 6b). A number of long-range contacts are observed in the spectra of Figure 6a, defining the spatial proximity of the first α-helix ($\alpha_1$) and part of the $\beta$-sheet comprising strands $\beta_3$ and $\beta_4$, forming one of the structural subunits of the BRP monomer.[31] The additional amino acid-type selection filter clearly provides a gain in spectral resolution by dispersing the NOE peaks along the additional $AA_j$ dimension. This allows, for example, to distinguish the cross-peak between the methyls of Val20$_{\gamma 2}$ and Ala39 (highlighted by bold letters in Figure 6a) from the strong diagonal peak, although both methyl $^{13}$C have very similar resonance frequencies. For the BRP$-$Blm complex, the high spectral resolution allowed unambiguous and straightforward assignment of most of the observed methyl NOEs in the $(3_{cs} + 1_{aa})$-D spectrum.

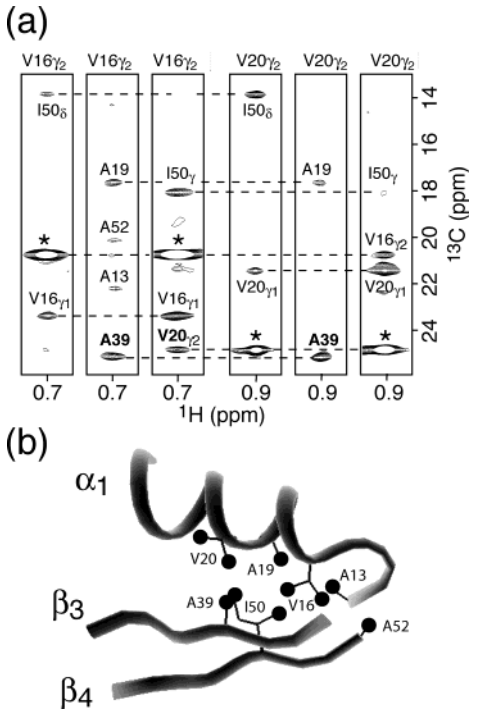


***Figure 6.*** (a) ($C_i$, $H_j$) strips extracted from a $(3_{cs} + 1_{aa})$-D methyl NOESY spectrum recorded for the BRP$-$Blm complex. The spectrum was recorded with the pulse sequence of Figure 1a and the insert of Figure 1c. The NOE mixing time was set to 100 ms. The strips were taken at the $C_j$ frequencies of valine methyls V16$_{\gamma 2}$ and V20$_{\gamma 2}$ and from different $AA_i$ planes. Only $AA_i$ planes with detected NOE peaks are shown. Diagonal peaks are marked by a star, and cross-peaks detected at ($C_i$, $AA_j$) are assigned to the corresponding methyl group. The methyl NOEs detected in (a) define a hydrophobic patch formed by helix $\alpha_1$, and the two strands $\beta_3$ and $\beta_4$ shown in (b). The schematic representation was derived from the X-ray structure of the BRP dimer[31] using the INSIGHT software (Accelrys).

If sensitivity allows for a second CT $^{13}$C-evolution period (insert of Figure 1b), amino acid-type selection for both proximal methyls further increases spectral resolution. Because sensitivity may be increased by the use of higher field spectrometers and cryogenic probes, the high spectral resolution provided by the new amino acid-type edited NOESY experiment may become particularly helpful for measuring a set of unambiguous long-range distances for larger molecular systems.

## Conclusions

Methyl groups are valuable probes of molecular structure and dynamics. It is therefore important to have NMR tools to record high-resolution spectra of methyl groups. Here, a new NMR filter sequence has been presented that allows amino acid-type editing of methyls in $^1$H$-^{13}$C correlation experiments. This filter presents a spectroscopic alternative to expensive and time-consuming amino acid-type-specific isotope labeling of the protein to increase spectral resolution. As a particular important

(31) Dumas, P.; Berdoll, M.; Cagnon, C.; Masson, J.-M. *EMBO J.* **1994**, *13*, 2483−2492.
(32) Shaka, A. J.; Pines, A. *J. Magn. Reson.* **1987**, *71*, 495−503.
(33) Shaka, A. J.; Keeler, J.; Frenkiel, T.; Freeman, R. *J. Magn. Reson.* **1983**, *52*, 335−338.
(34) Kupce, E.; Freeman, R. *J. Magn. Reson.* **1993**, *105A*, 234−238.
(35) Tycko, R.; Pines, A.; Gluckenheimer, R. *J. Chem. Phys.* **1985**, *83*, 2775−2802.

application of this filter, we have introduced new NMR experiments to record ($n_{cs} + n_{aa}$)-dimensional methyl−methyl correlation spectra for NOE measurements. These experiments present interesting new features for application to small and large molecules. We have shown that ($2_{cs} + 2_{aa}$)-D NOESY experiments are most appropriate for fast methyl−methyl NOE measurement in smaller proteins. Fast acquisition schemes are especially important in the context of high-throughput structural genomics or the study of unstable molecular systems by NMR. Higher-dimensional ($3_{cs} + 1_{aa}$)-D or ($3_{cs} + 2_{aa}$)-D NOESY spectra provide the high resolution required for unambiguous NOE assignment of larger proteins, which is a crucial step for protein fold determination by NMR. We therefore expect that the methyl NOESY experiments proposed here will become widespread in liquid-state NMR of proteins.

**Acknowledgment.** This work was supported by the Commissariat à l′Energie Atomique and the Centre National de la Recherche Scientifique. We thank B. Bersch, E. Rossy, and J. Covès for the preparation of the MerAa sample, and C. Vanbelle, M.-H. Rémy, and J.-M. Masson for the BRP−Blm sample. H.V.M. acknowledges the receipt of a fellowship from the C.E.A.

**Supporting Information Available:** One figure illustrating sideband suppression for $C^{next}$-decoupling during real-time $^{13}C$ labeling using a time-shifted decoupling sequence for alternating scans. This material is available free of charge via the Internet at http://pubs.acs.org.

JA0489644